Journal of Materials Chemistry A

PAPER

View Article Online
View Journal | View Issue

Cite this: J. Mater. Chem. A, 2017, 5, 10430

A novel naphthyl side-chained benzodithiophene polymer for efficient photovoltaic cells with a high fill factor of 75%†

Dakang Ding,‡[ab] Jiuxing Wang,‡[bd] Zurong Du,[b] Feng Li,[c] Weiye Chen,[a] Fushuai Liu,[a] Haiyan Li,[a] Mingliang Sun*[a] and Renqiang Yang*[b]

Received 5th March 2017
Accepted 25th April 2017

DOI: 10.1039/c7ta01994g

rsc.li/materials-a

To study which strategy (extending side chain p-conjugation with single-bonded or fused aromatic rings) is more effective in improving the photovoltaic properties of benzodithiophene (BDT)-based polymers, naphthyl (NP) and biphenyl (BP) units were introduced to the BDT core as conjugated side chains. Two polymers PBDTNP-DTBO and PBDTBP-DTBO based on NP or BP-substituted BDT and 5,6-bis(octyloxy)-4,7-di(thiophen-2-yl)benzo[*c*][1,2,5]oxadiazole (DTBO) were designed. These two polymers only exhibited small differences in the chemical structure, but great differences in photovoltaic performance. PBDTNP-DTBO showed a high power conversion efficiency (PCE) of 8.79%, with an open-circuit voltage (V_{oc}) of 0.82 V, a short-circuit current density (J_{sc}) of 14.34 mA cm^{-2}, and a fill factor (FF) of 74.73%, while PBDTBP-DTBO only showed a maximum PCE of 6.69%, with a V_{oc} of 0.75 V, a J_{sc} of 13.55 mA cm^{-2}, and a FF of 65.86%. Hence, extending the side chain p-conjugation system of a BDT-based polymer with naphthyl is a more effective method to enhance the photovoltaic properties.

Introduction

The past 30 years have witnessed the great progress achieved in the 珡eld of polymer solar cells (PSCs) and the power conversion efficiency (PCE) has exceeded 10%.[1–3] The development of polymer donors is a key driving force for the advances of PSCs. To realize high PCE, a polymer donor should have suitable energy levels, high hole mobility and good miscibility with the acceptor.[4,5] Many strategies have been developed to design high-performance polymer donors, such as introducing 珠uorine substituents and extending p-conjugated systems.[6–16] Compared with introducing 珠uorine substituents, extending p-conjugation systems is more environmentally friendly.

Among various donor units, benzo[1,2-*b*:4,5-*b*′]dithiophene (BDT) arouses particular interest due to its good planarity and strong p–p interaction. Extending the side chain p-conjugation system of BDT is an effective way to improve the photovoltaic properties of BDT-based polymers. In 2011, Hou and co-workers designed a two-dimensional (2D) conjugated BDT unit BDTT by replacing alkoxy groups with alkylthienyl groups.[17] The BDTT-based polymers exhibited simultaneously increased open-circuit voltage (V_{oc}), short-circuit current density (J_{sc}) and PCE values than BDT-based polymers. Given the success of designing BDTT, more BDT derivatives with larger side chain p-conjugation systems are synthesized by the introduction of single-bonded or fused aromatic rings into BDT.[15,16,18–27] In 2014, Wang *et al.* designed a novel donor unit BDTBzT by introducing two benzo[*b*]thiophene groups into BDT.[16] The BDTBzT-based polymer exhibited a much enhanced PCE (7.30%) than the BDT-based polymer (5.35%). Then Han *et al.* reported a polymer based on a BDT derivative with phenylthiophene groups as side chains.[27] The polymer showed a maximum PCE of 7.68%. Previous reports show that the photovoltaic properties can be improved through the introduction of single-bonded or fused aromatic rings into BDT. What is the difference in performance between these two methods? Which method is more effective? These issues need further study.

Diphenyl BDT (BDTP) is a widely used donor unit in constructing D–A polymers. Through introducing 珠uorine into the 珠anking benzene ring of BDTP, the highest PCE of BDTP-based polymers reached 9.02%.[9] Although the photovoltaic performance can be greatly enhanced by the introduction of 珠uorine, this method is costly and environmentally unfriendly. To date, extending the side chain p-conjugation system of BDTP has not

[a]Institute of Materials Science and Engineering, Ocean University of China, Qingdao 266100, China. E-mail: mlsun@ouc.edu.cn

[b]CAS Key Laboratory of Bio-based Materials, Qingdao Institute of Bioenergy and Bioprocess Technology, Chinese Academy Science, Qingdao 266101, China. E-mail: yangrq@qibebt.ac.cn

[c]Key Laboratory of Rubber-Plastics of Ministry of Education/Shandong Province, School of Polymer Science and Engineering, Qingdao University of Science & Technology, 53 Zhengzhou Road, Qingdao 266042, China

[d]Institute of Hybrid Materials, College of Materials Science and Engineering, Qingdao University, Qingdao 266071, China

† Electronic supplementary information (ESI) available. See DOI: 10.1039/c7ta01994g

‡ These authors contributed equally to this work.

been reported. Naphthalene is an extended conjugated structure based on phenyl, and it is fused together by two benzene units and all ten carbon atoms of naphthalene are in the same plane. Every hexatomic ring of naphthalene has alternating single and double connection, so the p-conjugation system can be expanded along the whole naphthalene structure. A biphenyl unit is another extending conjugated structure based on phenyl. Here, we designed two BDT derivatives, BDTNP and BDTBP, by introducing naphthyl and biphenyl into BDT, respectively.

Di(thiophen)-benzooxadiazole and di(thiophen)-benzothiadizole are two main electron-withdrawing units for constructing D–A copolymers with 2D BDT. A deeper HOMO level and increased planarity based on DTBO polymers can be achieved due to the higher electronegativity of oxygen atom and S⋯O interaction between thiophene and benzothiadizole. Therefore, 5,6-bis(octyloxy)-4,7-di(thiophen-2yl)benzo[*c*][1,2,5]oxadiazole (DTBO) was chosen as the acceptor unit. The optoelectronic properties of the two polymers based on BDTNP (named PBDTNP-DTBO) and BDTBP (named PBDTBP-DTBO) were thoroughly studied. PBDTNP-DTBO showed a high PCE of 8.79%, with a V_{oc} of 0.82 V, a J_{sc} of 14.34 mA cm^{-2}, and a 珡ll factor (FF) of 74.73%, while PBDTBP-DTBO only showed a maximum PCE of 6.69%, with a V_{oc} of 0.75 V, a J_{sc} of 13.55 mA cm^{-2}, and a FF of 65.86%.

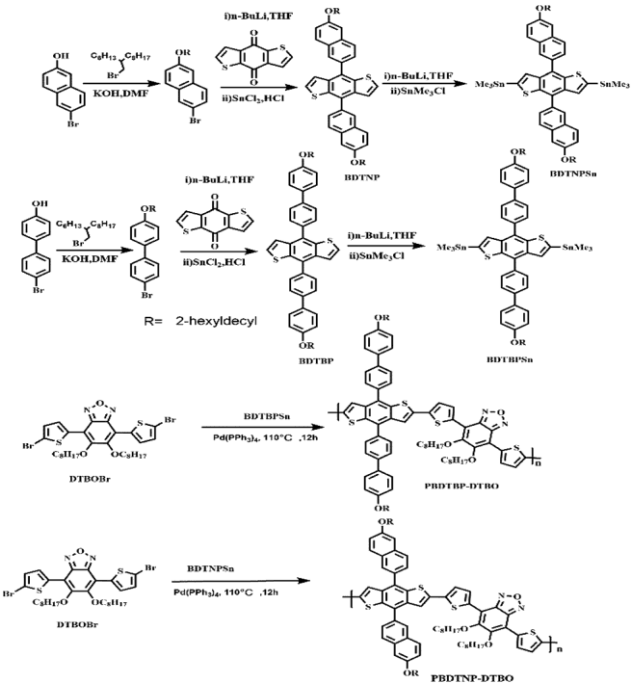

Scheme 1 Synthetic routes of BDTBP, BDTNP and their polymers.

Results and discussion

Synthesis and characterization

The synthetic routes for these new monomers (BDTNPSn and BDTBPSn) and polymers (PBDTBP-DTBO and PBDTNP-DTBO) are shown in Scheme 1 and the detailed synthetic processes are given in the Experimental section. Compound 4,8-dihydrobenzo[1,2-*b*:4,5-*b*′]dithiophen-4,8-dione, DTBOBr and 5-(bromomethyl)pentadecane were synthesized according to the reported methods.[16,28,29] The polymers were synthesized by the Stille coupling reaction with DTBOBr and BDTNPSn or BDTBPSn as reactants using tris(dibenzylideneacetone)dipalladium ($Pd_2(dba)_3$) and tri(*o*-tolyl)phosphine (P(*o*-tol)$_3$) as catalysts in anhydrous toluene at 110 °C. These polymers both exhibited poor solubility, and could be dissolved in hot *o*-dichlorobenzene (DCB). The number-average molecular weight (M_n) of PBDTNP-DTBO determined by gel permeation chromatography (GPC) with trichlorobenzene as the eluent at 150 °C was 56 kDa with the polydispersity index (PDI) of 1.98, while the M_n of PBDTBP-DTBO was 43 kDa with the PDI of 2.31. The thermal properties of the polymer were recorded by thermogravimetric analysis at a heating rate of 10 °C min^{-1} under a nitrogen atmosphere. As shown in Fig. S1 (ESI),† the onset decomposition temperature (5% weight loss) of the polymer PBDTNP-DTBO and PBDTBP-DTBO was 322.5 and 326.3 °C, respectively, which were enough for application in PSCs.

Optical properties

The ultraviolet-visible absorption (UV-vis) spectra of PBDTNP-DTBO and PBDTBP-DTBO in thin 珡lms and dilute DCB solution are shown in Fig. 1a. These two polymers exhibited very similar absorption spectra both in 珡lms and solution. In thin 珡lms, the shoulder peaks of PBDTNP-DTBO and PBDTBP-DTBO located at 638 nm and 635 nm were attributed to the aggregations of the polymer chains. The absorption peak wavelength of

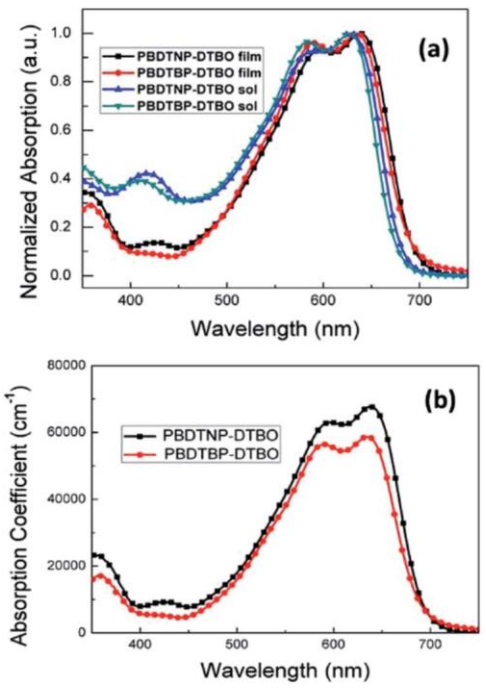

Fig. 1 (a) Normalized absorption spectra of PBDTNP-DTBO and PBDTBP-DTBO in DCB solution and as solid films at room temperature. (b) Absorption coefficients of PBDTNP-DTBO and PBDTBP-DTBO.

PBDTNP-DTBO and PBDTBP-DTBO was *ca.* 596 nm and 589 nm, respectively, which could be attributed to the intramolecular charge transfer between the DTBO unit and the BDT unit. Compared with the absorption spectra in thin 珡lms, the two polymers in dilute DCB solution showed slightly blue-shi测ed spectra. The detailed optical data are listed in Table 1. The absorption onset (l_{onset}) of the polymer PBDTNP-DTBO and PBDTBP-DTBO was 705 and 703 nm, respectively. Hence, according to the equation E_g^{opt} ¼ 1240/l onset, the optical band gaps (E_g^{opt}) of the two polymers were both 1.76 eV. As shown in Fig. 1b, the maximum 珡lm absorption coefficients of PBDTNP-DTBO and PBDTBP-DTBO were 6.74×10^4 and 5.76×10^4 cm^{-1}, respectively, indicating that PBDTNP-DTBO has stronger ability of harvesting light, which may be one reason for the increased photovoltaic performance of PBDTNP-DTBO.

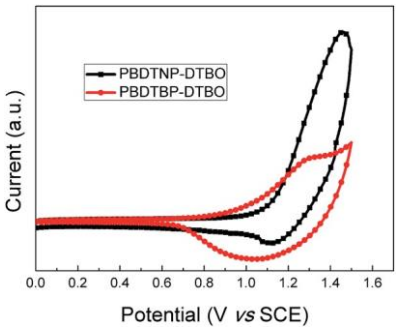

Fig. 2 Electrochemical cyclic voltammograms of the two polymers.

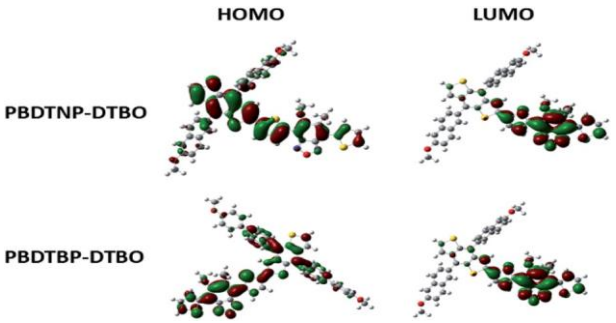

Fig. 3 Optimized molecular geometries and frontier molecular orbitals for PBDTNP-DTBO and PBDTBP-DTBO obtained by DFT calculations.

Electrochemical properties

The electrochemical properties of PBDTNP-DTBO and PBDTBP-DTBO were studied by cyclic voltammetry (CV).The CV curves are shown in Fig. 2 and the detailed onset oxidation potentials (E_{ox}) and HOMO and LUMO energy levels are listed in Table 1. The E_{ox} of PBDTNP-DTBO and PBDTBP-DTBO was 1.12 and 0.92 V respectively, *vs.* the saturated calomel electrode (SCE). The half-wave potential of the ferrocene/ferrocenium (Fc/Fc^+) redox couple was used as the internal standard, and the potential ($E_{1/2}^{(Fc/Fc+)}$) *vs.* the SCE was measured to be 0.40 V. The HOMO energy levels of PBDTNP-DTBO and PBDTBP-DTBO calculated by the equation E_{HOMO} ¼ —e(E_{ox} + 4.8 $_{T/2}E^{(Fc/Fc+)}$) were —5.52 and —5.32 eV, respectively. Higher V_{oc} of PBDTNP-DTBO based polymer solar cells could be achieved due to the low-lying HOMO. As shown in Fig. S2,† the LUMO was obtained by the E_{re} and the detailed energy level values are listed in Table 1. Compared with BDTBP, the BDTNP with fused aromatic rings exhibits a larger p-conjugation side chain system on account of the zero torsion angle on phenyl units. Fused aromatic rings (NP) may decrease the electron density of BDT units more effectively due to the phenyl unit with high ionization potential and low electron densities, so BDTNP could become more electron-withdrawing relative to BDTBP, which would lead to a lower-lying HOMO energy level.

Theoretical calculations

To further research the optoelectronic properties about the HOMO and LUMO of PBDTNP-DTBO and PBDTBP-DTBO, density functional theory (DFT) calculations were carried out using the Gaussian 09 program in the gas phase. In order to reduce calculation time, some simpli珡ed methods were carried out, such as choosing one repeating unit and replacing alkyl side chains with methyl groups. The optimized molecular geometries were recognized as the minimum-energy conformations by vibrational calculations at the same level. The optimized molecular geometry and frontier molecular orbitals are shown in Fig. 3 and the detailed energy levels are listed in Table 1. The simulated energy levels calculated from the DFT calculations were well consistent with the experimental results estimated from the CV curves. As shown in Fig. S3,† PBDTNP-DTBO exhibited a larger side chain and backbone dihedral angles than PBDTBP-DTBO, which may account for the deeper HOMO and LUMO energy levels of PBDTNP-DTBO relative to PBDTBP-DTBO. These two polymers exhibited similar distributions of HOMO and LUMO. The LUMO was mainly delocalized in the DTBO unit, while the HOMO was located in both BDT and DTBO units.

Photovoltaic properties and hole mobility

To study the photovoltaic properties of these two polymers, bulk heterojunction PSCs were fabricated with a traditional structure

Table 1 Optical absorption properties and molecular energy levels of the two polymers

Polymer	l_{max} 珡lm (nm)	l_{max} solution (nm)	l_{onset} 珡lm (nm)	E_g^{opt} (eV)	E_{ox} (eV)	$HOMO^{cv}$ (eV)	$LUMO^{cv}$ (eV)	E_g^{DFT} (eV)	$HOMO^{DFT}$ (eV)	$LUMO^{DFT}$ (eV)
PBDTNP-DTBO	424, 596, 638	420, 592, 628	705	1.76	1.12	—5.52	—3.21	2.48	—5.13	—2.65
PBDTBP-DTBO	413, 589, 635	411, 585, 627	703	1.76	0.92	—5.32	—3.08	2.39	—4.96	—2.57

of indium tin oxide (ITO)/poly(3,4-ethylene dioxythiophene):-poly(styrenesulfonate) (PEDOT:PSS)/polymer:$PC_{71}BM$/Ca/Al. The active layer solutions with different polymer:$PC_{71}BM$ (D : A) ratios were stirred at 120 °C for 2 h. All PSCs were tested under the illumination of AM 1.5 G, 100 mW cm^{-2}.

The current density–voltage (*J*–*V*) curves of the PSCs based on different D : A ratios are shown in Fig. 4 and their detailed parameters are listed in Table 2. As can be seen from Table 2, both PBDTNP-DTBO and PBDTBP-DTBO showed the best photovoltaic performance when they were blended with $PC_{71}BM$ at the D : A ratio of 1 : 2. The best PCEs (7.70%, 8.79% and 7.81%) of PBDTNP-DTBO with different D : A ratios were all obviously higher than those (6.00%, 6.69% and 6.19%) of PBDTBP-DTBO. It is a pity that the PCE of the two polymers did not increase any more when processing additives were blended. PBDTNP-DTBO showed a highest PCE of 8.79%, with a V_{oc} of 0.82 V, a J_{sc} of 14.34 mA cm^{-2}, and a fill factor (FF) of 74.73%, while PBDTBP-DTBO only showed a maximum PCE of 6.69%, with a V_{oc} of 0.75 V, a J_{sc} of 13.55 mA cm^{-2}, and a fill factor (FF) of 65.86%. The V_{oc}, J_{sc} and FF for PBDTNP-DTBO were improved simultaneously in comparison with those for PBDTBP-DTBO. The enhancement of V_{oc} may result from the deeper HOMO energy level. The higher absorption coefficient of PBDTNP-DTBO should be one of the contributing factors for the improvement of J_{sc}. The FF of PBDTNP-DTBO-based PSCs was as high as 74.73%, which is a good result in the field of PSCs, and it may result from the excellent active layer morphology. These results indicated that extending the side chain p-conjugation system of BDTP through fused aromatic rings is better than through single-bonded aromatic rings for PSCs.

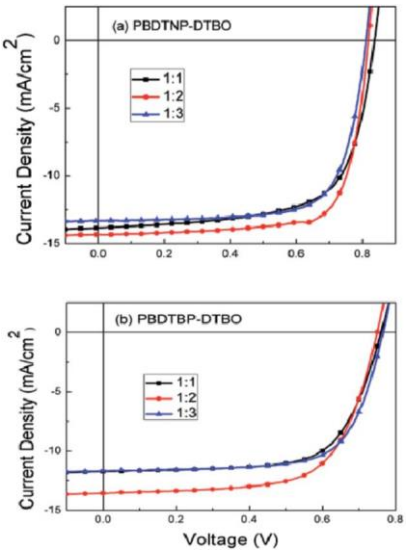

Fig. 4 *J*–*V* characteristics of the PSCs based on (a) PBDTNP-DTBO and (b) PBDTBP-DTBO with different polymer/$PC_{71}BM$ ratios.

Table 3 Comparison of the photovoltaic parameters of DTBO-based polymers

Polymer	V_{oc} (V)	J_{sc} (mA cm^{-2})	FF (%)	PCE (%)	Reference
PBDTNP-DTBO	0.82	14.34	74.73	8.79	This work
PBDTBP-DTBO	0.75	13.55	65.86	6.69	This work
PBO-*m*-FPO	0.87	14.3	64	8.0	30
PBDTTTBO	0.85	11.8	59	5.9	31
P3	0.86	10.8	59	5.5	32
PQDT-DTPyT	0.75	13.49	55.1	5.57	33
PIPCP	0.86	13.4	53	6.13	34
PBPT-12	0.75	12.56	54.2	5.11	35

Table 3 summarizes the photovoltaic parameters of DTBO-based polymers. The previously reported highest PCE for DTBO-based polymers is 8.0%, with a V_{oc} of 0.87 V, a J_{sc} of 14.3 mA cm^{-2}, and an FF of 64%.[30] However, the polymer contains fluorine atoms which are detrimental to the environment. This work indicates that extending the side chain p-conjugation system with the naphthyl side group is a more effective and environmentally friendly method.

The hole mobility was measured by the space-charge-limited-current (SCLC) method with the device structure of ITO/PEDOT:PSS/polymer:$PC_{71}BM$/MoO_3/Al. As shown in Fig. S4,† the hole mobility of PBDTNP-DTBO and PBDTBP-DTBO is 2.65×10^{-4} and 2.30×10^{-4} $cm^2 V^{-1} s^{-1}$, respectively. The polymer PBDTNP-DTBO exhibited higher hole mobility than PBDTBP-DTBO, which may be part of the reason that the PBDTNP-DTBO-based PSC device showed higher J_{sc} and FF.[5]

The external quantum efficiency (EQE) spectra of the optimized PSCs based on PBDTNP-DTBO and PBDTBP-DTBO are shown in Fig. 5. The EQEs of PBDTNP-DTBO based PSC devices were higher than those of PBDTBP-DTBO in the region of 400–700 nm, which should be another reason that PBDTNP-DTBO-based devices showed higher J_{sc}. The calculated current densities integrated from the EQE curves of PBDTNP-DTBO and PBDTBP-DTBO were 14.01 and 13.14 mA cm^{-2}, respectively, which were consistent with the J_{sc} obtained by *J*–*V* curves.

Table 2 Photovoltaic properties of PBDTNP-DTBO and PBDTBP-DTBO with different polymer:$PC_{71}BM$ (D : A) ratios

Polymer	D : A	V_{oc} (V)	J_{sc} (mA cm^{-2})	FF (%)	PCE_{max}/PCE_{ave} (%)
PBDTNP-DTBO	1 : 1	0.83	12.88	72.06	7.70/7.63
PBDTNP-DTBO	1 : 2	0.82	14.34	74.73	8.79/8.68
PBDTNP-DTBO	1 : 3	0.81	13.31	72.46	7.81/7.72
PBDTBP-DTBO	1 : 1	0.76	11.75	67.21	6.00/5.94
PBDTBP-DTBO	1 : 2	0.75	13.55	65.86	6.69/6.65
PBDTBP-DTBO	1 : 3	0.76	11.81	68.60	6.19/6.10

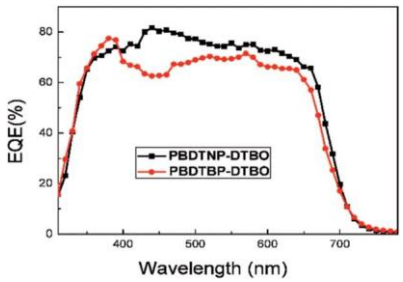

Fig. 5 EQE spectra of the PSCs based on PBDTNP-DTBO and PBDTBP-DTBO.

Active layer morphology

To investigate the morphology of the active layer, atomic force microscopy (AFM) and transmission electron microscopy (TEM) measurements were carried out. As shown in Fig. 6, the PBDTBP-DTBO:$PC_{71}BM$ 珡lm showed a much rougher surface than the PBDTNP-DTBO:$PC_{71}BM$ 珡lm. The root-mean-square (RMS) surface roughness values were 2.38 and 0.99 nm for PBDTBP-DTBO:$PC_{71}BM$ and PBDTNP-DTBO:$PC_{71}BM$, respectively. According to the literature, the rougher surface is unfavourable to realizing a high PCE.[5] The TEM images clearly show that the phase separation of PBDTBP-DTBO:$PC_{71}BM$ was very serious. As the exciton diffusion length is only rv10–20 nm, large phase separation is detrimental to the separation of excitons. In contrast, the PBDTNP-DTBO:$PC_{71}BM$ 珡lm showed a much smaller phase separation with nanoscale domains. From the AFM and TEM results, we can conclude that the compatibility of PBDTNP-DTBO:$PC_{71}BM$ was much better than that of PBDTBP-DTBO:$PC_{71}BM$. Polymer PBDTNP-DTBO exhibited a higher regularity, higher molecular weight and more effective extended p-conjugation system caused by the less torsion angle of the side chain, which may be potential factors to in珠uence the morphology. A better active layer morphology should be another factor for the improvement of J_{sc} and FF for PBDTNP-based PSCs.

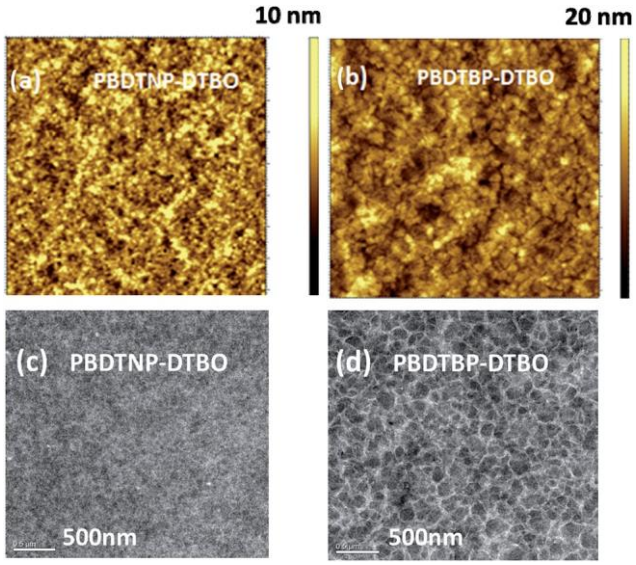

Fig. 6 AFM (a and b) and TEM (c and d) images of polymer:$PC_{71}BM$ blends. The size of the AFM images is 5 mm × 5 mm.

Conclusions

In summary, two novel BDT-based polymers containing naphthyl (PBDTNP-DTBO) and biphenyl (PBDTBP-DTBO) side chains were synthesized, and their optoelectronic properties were studied in detail. Compared with PBDTBP-DTBO, PBDTNP-DTBO exhibited a larger 珡lm absorption coefficient, deeper HOMO and LUMO, improved EQE, and better miscibility with $PC_{71}BM$. As a result, the photovoltaic properties of PBDTNP-DTBO were greatly improved and the maximum PCE achieved was 8.79%. This work indicated that extending the side chain p-conjugation system of a BDT-based polymer with naphthyl is a more effective method to enhance the photovoltaic properties.

Experimental section

Materials

All chemicals and solvents were purchased from commercial sources. Toluene and tetrahydrofuran (THF) were dried using sodium under an argon atmosphere before used for sensitive reactions and the other solvents were used directly. Compound 4′-bromo biphenyl-4-ol and 6-bromona phthalen-2-ol were purchased from J & K. Compound benzo[1,2-*b*:4,5-*b*′] dithiophen-4,8-dione, DTBOBr, BDTBPSn and 5-(bromomethyl)pentadecane were synthesized according to the reported methods.[16,28,29] The new monomer BDTNP and the corresponding polymers were synthesized in accordance with Scheme 1 and the detailed synthetic routes are as follows.

Synthesis of compound 2-bromo-6-(2-hexyldecyloxy) naphthalene

A mixture of 6-bromonaphthalen-2-ol (4.46 g, 20 mmol), 5-(bromomethyl)pentadecane (9.16 g, 30 mmol), potassiumhydroxide (1.68 g, 30 mmol) and dimethyl formamide (DMF, 50 mL) was stirred at 100 °C for 24 hours. A珌er cooling the 珠ask to room temperature, 40 mL water was added to dissolve the white inorganic substance. The mixture was extracted with hexane several times, and the organic phase was dried using anhydrous Na_2SO_4. A珌er removing the solvent under reduced pressure, the crude product was puri珡ed further by silica column chromatography using petroleum ether as the eluent. The colorless oil was received (5.83 g, 65.14% yield).

^{1}H NMR (600 MHz, $CDCl_3$): d 7.90 (d, 1H), 7.63 (d, 1H), 7.57 (d, 1H), 7.49–7.46 (dd, 1H),7.17–7.14 (dd, 1H), 7.08 (d, 1H), 3.93 (d, 2H), 1.85–1.80 (m, 1H), 1.43–1.22 (m, 24H), 0.88 (m, 6H).

Synthesis of compound BDTNP

Compound 2-bromo-6-(2-hexyldecyloxy)naphthalene (5.61 g, 12.54 mmol) was dissolved in THF (30 mL) and then was cooled to −78 °C under an argon atmosphere. *n*-Butyllithium solution (8.36 mL, 1.6 mol L^{-1}, 13.78 mmol) was added dropwise into the 珠ask. The mixture was maintained at this temperature for two

hours, and then benzo[1,2-*b*:4,5-*b*′]dithiophen-4,8-dione (0.92 g, 4.18 mmol) was quickly poured into the flask. After keeping the reaction at −78 °C for another hour, the temperature of the mixture was increased to room temperature and stirred overnight. $SnCl_2\$2H_2O$ in 10% HCl bubbled using argon was injected into the reaction. The solution was stirred at 70 °C for 4 hours and the cooled mixture was poured into 20 mL water. The mixture was extracted with diethylether and a white solid (1.8 g, 47.3% yield) was obtained after further purification by column chromatography using dichloromethane and petroleum ether as the eluents.

^{1}H NMR (600 MHz, $CDCl_3$): δ 8.13 (s, 2H), 7.92 (d, 2H), 7.83 (d, 2H), 7.80–7.75 (dd, 2H), 7.42 (d, 2H), 7.36 (d, 2H), 7.25 (s, 2H), 7.23 (d, 2H), 4.02 (d, 4H), 1.94–1.86 (m, 2H), 1.55–1.25 (m, 48H), 0.92–0.87 (m, 12H).

^{13}C HMR (150 MHz, $CDCl_3$): δ 158.02, 138.51, 136.41, 134.46, 134.36, 130.48, 129.71, 129.05, 128.29, 127.82, 127.34, 127.25, 123.08, 119.77, 106.59, 71.09, 37.70, 31.94, 31.91, 31.50, 31.49, 30.08, 29.75, 29.64, 29.37, 26.88, 22.71, 14.15.

Synthesis of compound BDTNPSn

Compound BDTNP (1.84 g, 1.99 mmol) was dissolved in anhydrous THF (40 mL) under an argon atmosphere, and then *n*-butyllithium (3.36 mL, 5.37 mmol, 1.6 mol L^{-1}) was dropped slowly at 0 °C. After the mixture stirred at room temperature for 1 hour, trimethyltin chloride (6.96 mL, 6.96 mmol, 1.0 mol L^{-1}) was injected into the flask quickly. The mixture was stirred at room temperature overnight and 10 mL water was poured into the flask. The mixture was extracted with diethylether and then the solvent was removed under reduced pressure. The raw product can be purified by recrystallization from acetone, and a white solid (1.5 g, 48% yield) could be received.

^{1}H NMR (600 MHz,$CDCl_3$): δ 8.14 (s, 2H), 7.93 (d, 2H), 7.84 (d, 2H), 7.80 (dd, 2H), 7.40 (m, 2H), 7.27 (d, 2H), 7.24 (dd, 2H), 4.02 (d, 4H), 1.94–1.86 (m, 2H), 1.53–1.22 (m, 48H), 0.95–0.84 (m, 12H), 0.38–0.26 (m, 18H). ^{13}C NMR (150 MHz, $CDCl_3$): δ 157.89, 142.79, 142.11, 137.25, 135.12, 134.23, 130.75, 129.70, 128.95, 128.90, 128.25, 128.11, 127.12, 119.63, 106.52, 71.11, 37.96, 31.90, 31.48, 30.07, 29.74, 29.63, 29.36, 26.89, 26.87, 22.70, 14.14. HRMS (MALDI-TOF): calcd for: $C_{68}H_{98}O_2S_2Sn_2$ (M^+): 1248.505, found: 1248.663.

Synthesis of PBDTNP-DTBO and PBDTBP-DTBO

The mixture of BDTNSn (124.97 mg, 0.10 mmol), DTBOBr (69.86 mg, 0.10 mmol), Pd_2dba_3 (2.0 mg), P(*o*-tol)$_3$ (4.0 mg) and toluene (5 mL) was added into the flask under an argon atmosphere, which was heated to 110 °C and stirred overnight. The solution was dropped into methanol. The raw polymer was received by filtration and purified further by Soxhlet extraction with hexane, acetone, dichloromethane, and chloroform. The remaining solid was dissolved using *o*-dichlorobenzene at 80 °C, and then washed with *o*-dichlorobenzene by chromatography. It was dropped into methanol again before the solution was removed exactly. It was obtained as a blue solid (111.12 mg, 76% yield) after filtration.

Elemental analysis calcd (%) for $C_{92}H_{120}N_2O_5S_4$: C 75.57%, H 8.27%, found: C 75.43%, H 7.96%.

PBDTBP-BTBO was prepared by the same method, and a deep blue solid was obtained (104.4 mg, 69% yield).

Elemental analysis calcd (%) for $C_{96}H_{124}N_2O_5S_4$: C 76.14%, H 8.25%, found: C 76.03%, H 8.32%.

Characterization

^{1}H nuclear magnetic resonance (NMR) and ^{13}C NMR spectra were measured with a Bruker AVANCE-III 600 spectrometer using tetramethylsilane (TMS) as the internal reference. HRMS were performed on a Bruker time-of-flight mass spectrometer with the model of MALDI-TOF. The molecular weight and polydispersity were measured by gel permeation chromatography (GPC) analysis with an ELEOS system using trichlorobenzene as the eluent at 150 °C. Thermal gravimetric analysis (TGA) curves were obtained by using a STA-409 at a heating rate of 10 °C min^{-1}. Cyclic voltammetry (CV) curves were recorded by using a CHI660D electrochemical workstation using polymer films on glassy carbon as the working electrode, a saturated calomel as the reference electrode and a platinum wire as the counter electrode in the solution of tetrabutylammonium phosphorus hexafluoride (Bu_4NPF_6, 0.1 M) in acetonitrile at a scanning rate of 50 mV s^{-1}. UV-vis absorption spectra were recorded on a Hitachi U-4100 spectrophotometer. The absorption spectra of films were measured by quartz plates spin-coated from their chloroform solutions. The surface morphological characterization of films blended with polymers and PCBM were done by using a tapping-mode atomic force microscope Agilent 5400.

Fabrication and characterization of polymer solar cells

The polymer solar cell devices were fabricated on the glass substrates spin-coated with indium tin oxide (ITO) using a traditional sandwich structure of ITO/PEDOT:PSS/polymer:$PC_{71}BM$/Ca/Al. The active area for the solar cell devices was about 0.1 cm^2. The ITO coated glass substrates were cleaned in an ultrasonic bath with ITO detergent, deionized water, acetone, toluene, methanol and isopropanol, sequentially. The washed ITO glasses were treated with oxygen plasma for 20 minutes, and then they were spin-coated with *ca.* 40 nm film of PEDOT (poly(3,4-ethylene dioxythiophene)):PSS (poly(styrenesulfonate)) under an argon atmosphere. The active layer consisting of polymers and $PC_{71}BM$ (10 mg mL^{-1}) with different ratios of DIO were dissolved in deoxygenated anhydrous chloroform solution overnight and spin-cast onto the PEDOT:PSS layer. Finally, the negative electrode consisting of Ca (10 nm) and aluminum (100 nm) was thermally evaporated onto the active layer. The current density–voltage (*J*–*V*) curves were measured with a Keithley 2420 source measurement unit under simulated AM 1.5 G irradiation (100 mW cm^{-2}) from a Newport solar simulator. A calibrated silicon solar cell was used to determine the light intensity. The external quantum efficiency (EQE) of the PSC devices was measured with a certified Newport incident photon conversion efficiency (IPCE) measurement system.

Acknowledgements

The authors gratefully acknowledge 珍nancial support from the NSFC (51573205 and 21274134).

References

1 Y. Liu, J. Zhao, Z. Li, C. Mu, W. Ma, H. Hu, K. Jiang, H. Lin, H. Ade and H. Yan, *Nat. Commun.*, 2014, 5, 5293.
2 H. Yao, W. Zhao, Z. Zheng, Y. Cui, J. Zhang, Z. Wei and J. Hou, *J. Mater. Chem. A*, 2016, 4, 1708–1713.
3 Z. He, B. Xiao, F. Liu, H. Wu, Y. Yang, S. Xiao, C. Wang, T. P. Russell and Y. Cao, *Nat. Photonics*, 2015, 9, 174–179.
4 Y. Li, *Acc. Chem. Res.*, 2012, 45, 723–733.
5 J. Wang, X. Bao, D. Ding, M. Qiu, Z. Du, J. Wang, J. Liu, M. Sun and R. Yang, *J. Mater. Chem. A*, 2016, 4, 11729–11737.
6 Y. Wu, Z. Li, W. Ma, Y. Huang, L. Huo, X. Guo, M. Zhang, H. Ade and J. Hou, *Adv. Mater.*, 2013, 25, 3449–3455.
7 T. L. Nguyen, H. Choi, S. J. Ko, M. A. Uddin, B. Walker, S. Yum, J. E. Jeong, M. H. Yun, T. J. Shin, S. Hwang, J. Y. Kim and H. Y. Woo, *Energy Environ. Sci.*, 2014, 7, 3040–3051.
8 M. Zhang, X. Guo, S. Zhang and J. Hou, *Adv. Mater.*, 2014, 26, 1118–1123.
9 N. Wang, W. Chen, W. Shen, L. Duan, M. Qiu, J. Wang, C. Yang, Z. Du and R. Yang, *J. Mater. Chem. A*, 2016, 4, 10212–10222.
10 Y. Liu, W. Zhao, Y. Wu, J. Zhang, G. Li, W. Li, W. Ma, J. Hou and Z. Bo, *J. Mater. Chem. A*, 2016, 4, 8097–8104.
11 Y. Liu, G. Li, Z. Zhang, L. Wu, J. Chen, X. Xu, X. Chen, W. Ma and Z. Bo, *J. Mater. Chem. A*, 2016, 4, 13265–13270.
12 H. Zheng, J. Wang, W. Chen, C. Gu, J. Ren, M. Qiu, R. Yang and M. Sun, *J. Mater. Chem. C*, 2016, 4, 6280–6286.
13 Y. Deng, J. Liu, J. Wang, L. Liu, W. Li, H. Tian, X. Zhang, Z. Xie, Y. Geng and F. Wang, *Adv. Mater.*, 2014, 26, 471–476.
14 D. Ding, J. Wang, W. Chen, M. Qiu, J. Ren, H. Zheng, D. Liu, M. Sun and R. Yang, *RSC Adv.*, 2016, 6, 51419–51425.
15 J.-H. Kim, C. E. Song, B. Kim, I.-N. Kang, W. S. Shin and D.-H. Hwang, *Chem. Mater.*, 2014, 26, 1234–1242.
16 J. Wang, M. Xiao, W. Chen, M. Qiu, Z. Du, W. Zhu, S. Wen, N. Wang and R. Yang, *Macromolecules*, 2014, 47, 7823–7830.
17 L. Huo, S. Zhang, X. Guo, F. Xu, Y. Li and J. Hou, *Angew. Chem., Int. Ed.*, 2011, 50, 9697–9702.
18 J.-H. Kim, J. B. Park, I. H. Jung, S. C. Yoon, J. Kwak and D.-H. Hwang, *J. Mater. Chem. C*, 2015, 3, 4250–4253.
19 Z. Xiao, J. Subbiah, K. Sun, D. J. Jones, A. B. Holmes and W. W. H. Wong, *Polym. Chem.*, 2014, 5, 6710–6717.
20 H. Yao, H. Zhang, L. Ye, W. Zhao, S. Zhang and J. Hou, *Macromolecules*, 2015, 48, 3493–3499.
21 H.-S. Chung, W.-H. Lee, C. E. Song, Y. Shin, J. Kim, S. K. Lee, W. S. Shin, S.-J. Moon and I.-N. Kang, *Macromolecules*, 2014, 47, 97–105.
22 M. Bolognesi, D. Gedefaw, D. Dang, P. Henriksson, W. Zhuang, M. Tessarolo, E. Wang, M. Muccini, M. Seri and M. R. Andersson, *RSC Adv.*, 2013, 3, 24543.
23 J. Lee, J.-H. Kim, B. Moon, H. G. Kim, M. Kim, J. Shin, H. Hwang and K. Cho, *Macromolecules*, 2015, 48, 1723–1735.
24 C.-Y. Kuo, W. Nie, H. Tsai, H.-J. Yen, A. D. Mohite, G. Gupta, A. M. Dattelbaum, D. J. William, K. C. Cha, Y. Yang, L. Wang and H.-L. Wang, *Macromolecules*, 2014, 47, 1008–1020.
25 R. S. Kularatne, P. Sista, H. Q. Nguyen, M. P. Bhatt, M. C. Biewer and M. C. Stefan, *Macromolecules*, 2012, 45, 7855–7862.
26 R. S. Kularatne, F. J. Taenzler, H. D. Magurudeniya, J. Du, J. W. Murphy, E. E. Sheina, B. E. Gnade, M. C. Biewer and M. C. Stefan, *J. Mater. Chem. A*, 2013, 1, 15535.
27 L. Han, T. Hu, X. Bao, M. Qiu, W. Shen, M. Sun, W. Chen and R. Yang, *J. Mater. Chem. A*, 2015, 3, 23587–23596.
28 B. Liu, X. Chen, Y. Zou, L. Xiao, X. Xu, Y. He, L. Li and Y. Li, *Macromolecules*, 2012, 45, 6898–6905.
29 J. Hou, M.-H. Park, S. Zhang, Y. Yao, L.-M. Chen, J.-H. Li and Y. Yang, *Macromolecules*, 2008, 41, 6012–6018.
30 J. Yuan, Y. Zou, R. Cui, Y.-H. Chao, Z. Wang, M. Ma, Y. He, Y. Li, A. Rindgen, W. Ma, D. Xiao, Z. Bo, X. Xu, L. Li and C.-S. Hsu, *Macromolecules*, 2015, 48, 4347–4356.
31 J.-M. Jiang, P. Raghunath, H.-K. Lin, Y.-C. Lin, M. C. Lin and K.-H. Wei, *Macromolecules*, 2014, 47, 7070–7080.
32 I. V. Klimovich, D. K. Susarova, F. A. Prudnov, L. N. Inasaridze, O. A. Mukhacheva, A. V. Chernyak and P. A. Troshin, *Sol. Energy Mater. Sol. Cells*, 2016, 155, 378–386.
33 H. Zhou, L. Yang, S. C. Price, K. J. Knight and W. You, *Angew. Chem., Int. Ed.*, 2010, 49, 7992–7995.
34 M. Wang, H. Wang, T. Yokoyama, X. Liu, Y. Huang, Y. Zhang, T. Q. Nguyen, S. Aramaki and G. C. Bazan, *J. Am. Chem. Soc.*, 2014, 136, 12576–12579.
35 J. Yuan, X. Huang, H. Dong, J. Lu, T. Yang, Y. Li, A. Gallagher and W. Ma, *Org. Electron.*, 2013, 14, 635–643.